Supplementary Information

for:

Ditopic receptors containing urea groups for solvent extraction of Cu(II) salts

Israel Carreira-Barral,[a,b] Marta Mato-Iglesias,[a] Andrés de Blas,[a] Carlos Platas-Iglesias,[a] Peter A. Tasker,*[c] and David Esteban-Gómez*[a]

ESI Summary

Determination of the metal:ligand molar ratio by solvent extraction experiments

Experiments were carried out by contacting chloroform solutions (5 mL) of increasing concentration of the ligand (from 2×10^{-4} M to 10^{-3} M), with aqueous solutions (5 mL) of the appropriate metal salt ($CuSO_4$ or $CuCl_2$) at concentration of 10^{-3} M. The aqueous solutions were prepared from 2.5 mL of a 2×10^{-3} M metal salt solution, to which were added 2.5 mL of different mixtures of H_2SO_4-H_2O or HCl-H_2O solutions and the corresponding sodium salt solution (Na_2SO_4 or NaCl) to obtain the desired pH and a constant anion concentration (0.6 M). After vigorous stirring for 16 h at room temperature, the mixtures were separated and the equilibrium pH of the aqueous phase determined. Aliquots (1 mL) of the aqueous phase and organic phase were removed for copper analysis by ICP-OES. The aqueous phase was diluted to 10 mL in water and the organic phase was evaporated to dryness *in vacuo* and the residue re-dissolved in butan-1-ol (10 mL). Plots of the log of the distribution coefficient (log *D*) against log(ligand concentration) were generated to determine the metal:ligand molar ratio.

pH dependence of copper salt loading from acidic media

Experiments were carried out by contacting chloroform solutions (5 mL) of the appropriate ligand (10^{-3} M), with aqueous solutions (5 mL) of the appropriate metal salt, $CuSO_4$ or $CuCl_2$), (10^{-3} M) over a range of pH. The aqueous solutions were prepared from 2.5 mL of a $2x10^{-3}$ M copper salt solution, to which were added 2.5 mL of different mixtures of H_2SO_4-H_2O or HCl-H_2O solutions and the corresponding sodium salt solution (Na_2SO_4 or NaCl), altering the pH and keeping anion concentration constant at 0.6 M. Plots of the percentage of copper salt loaded against equilibrium pH were generated.

Effect of metal salt concentration in the feed solution on copper loading

A similar procedure to that above was followed, contacting 5 mL of ligand solutions (10^{-3} M) in chloroform with aqueous solutions (5 mL) of varied concentration of $CuSO_4$ or $CuCl_2$ at pH 5.5. The aqueous solutions were prepared from 2.5 mL of a 2×10^{-3} M copper salt solution, to which were added 2.5 mL of mixtures of $CuSO_4$ (0.1 M) or $CuCl_2$ (5×10^{-2} M) solutions and Na_2SO_4 or NaCl, altering the copper salt concentration and keeping anion concentration constant at 0.6 M. In this case, plots of percentage copper salt loading against copper salt concentration in the feed solution were generated.

Effect of anion concentration of the feed solution on copper loading

A similar procedure to that above was used. The aqueous solutions were prepared from 1 mL of a 5×10^{-3} M copper salt solution, to which was added 4 mL of mixtures of either Na_2SO_4 or NaCl solutions (0.2 M) and either H_2SO_4-H_2O or HCl-H_2O solutions to obtain the desired pH and a constant copper concentration equivalent to that of the ligand. Plots of percentage copper salt loading against anion concentration (SO_4^{2-} or Cl^-) in the feed solution were generated.

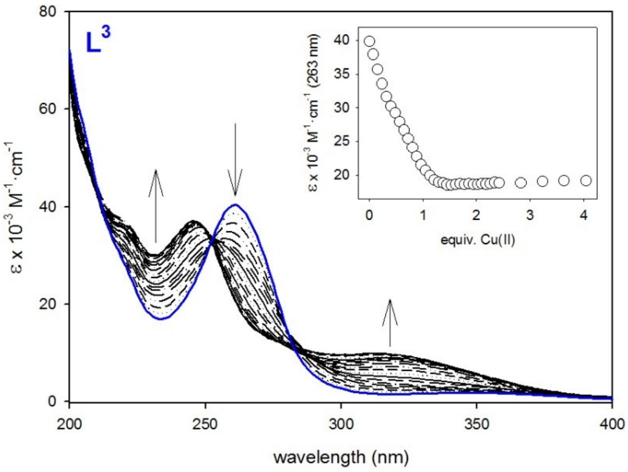

Figure S1. Family of UV/vis spectra recorded during the titration of $\mathbf{L^3}$ (10^{-5} M in DMSO) with a standard solution of $Cu(TfO)_2$ (10^{-3} M in dmso, 25 °C). Inset: titration profile at a selected wavelength *vs.* equivalents of Cu(II).

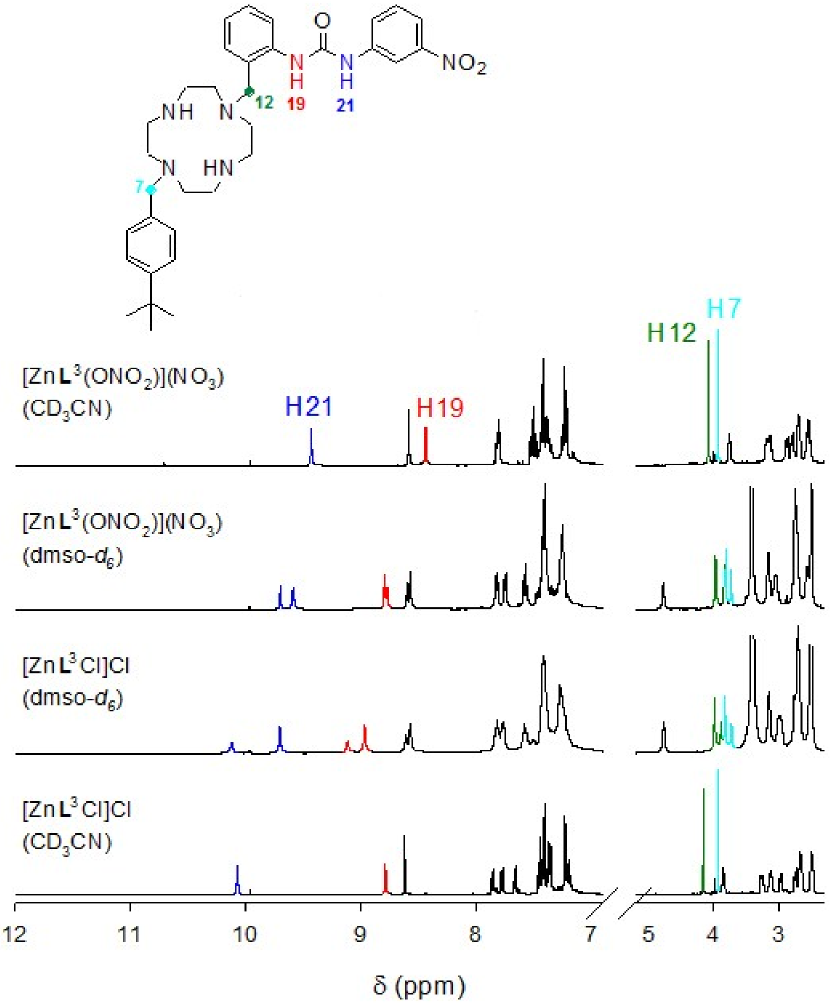

Figure S2. ^1H NMR spectra (300 MHz, dmso-d_6 and CD_3CN) of $[Zn\mathbf{L^3}(NO_3)](NO_3)$ and $[Zn\mathbf{L^3}Cl]Cl$ complexes and the atom labeling scheme used for those involved in interactions of anions with the metal-based receptor.

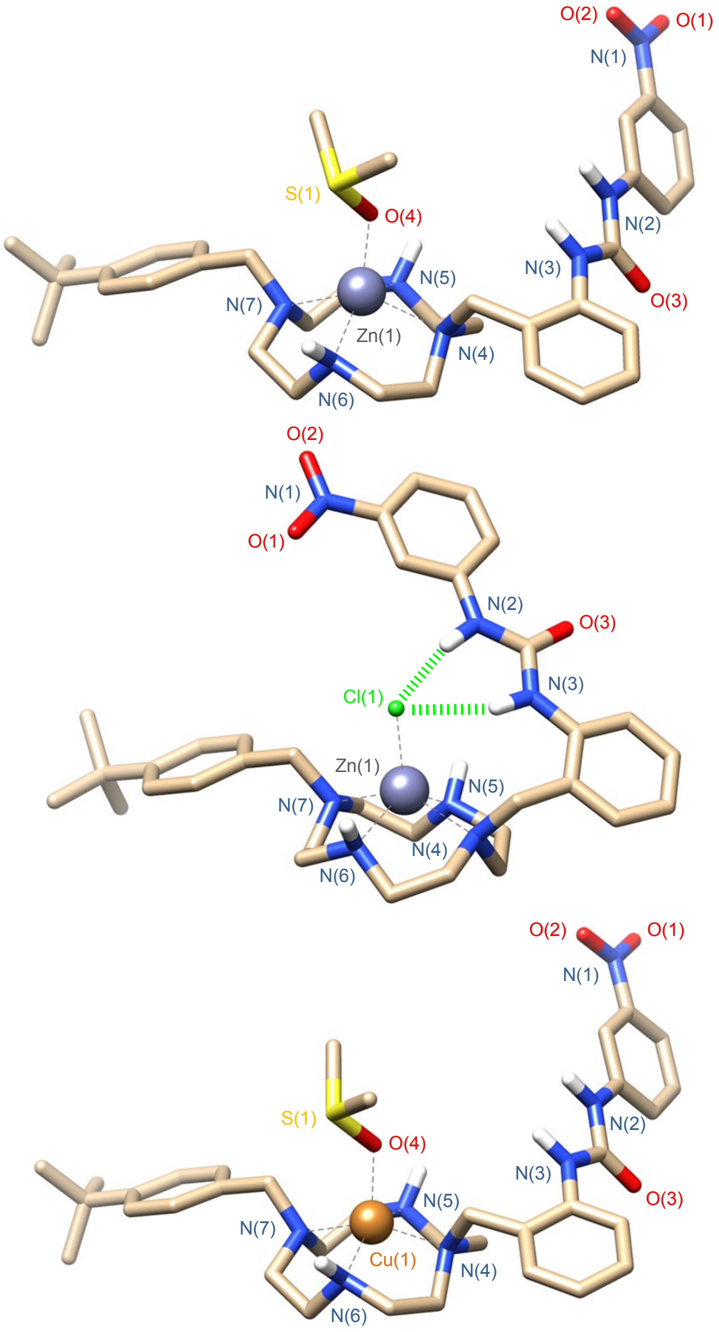

Figure S3. Geometries of the $[\mathrm{Zn}\mathbf{L}^3(\mathrm{OSMe}_2)]^{2+}$ (top), $[\mathrm{Zn}\mathbf{L}^3\mathrm{Cl}]^{+}$ (middle) and $[\mathrm{Cu}\mathbf{L}^3(\mathrm{OSMe}_2)]^{2+}$ (bottom) systems obtained from DFT calculations (TPSSh/SVP level) in dmso solution. Hydrogen atoms, except those involved in hydrogen-bonding interactions, are omitted for the sake of clarity.

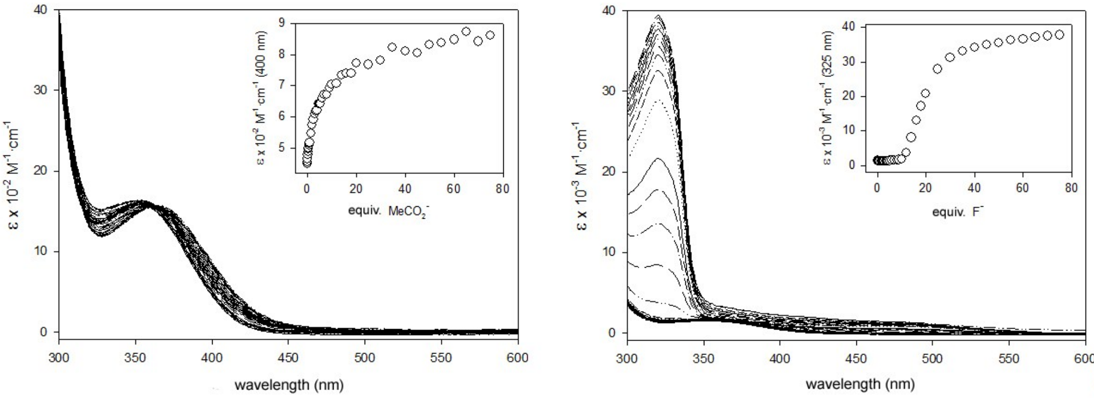

¶

Figure S4. Family of UV/vis spectra recorded during the titrations of **L**^{1} (10^{-4} M in dmso) with standard solutions of $[Bu_4N]\cdot MeCO_2$ (left) and $[Bu_4N]\cdot F$ (right) (10^{-2} M in DMSO, 25 °C). Inset: titration profiles at a selected wavelength *vs.* equivalents of anion.

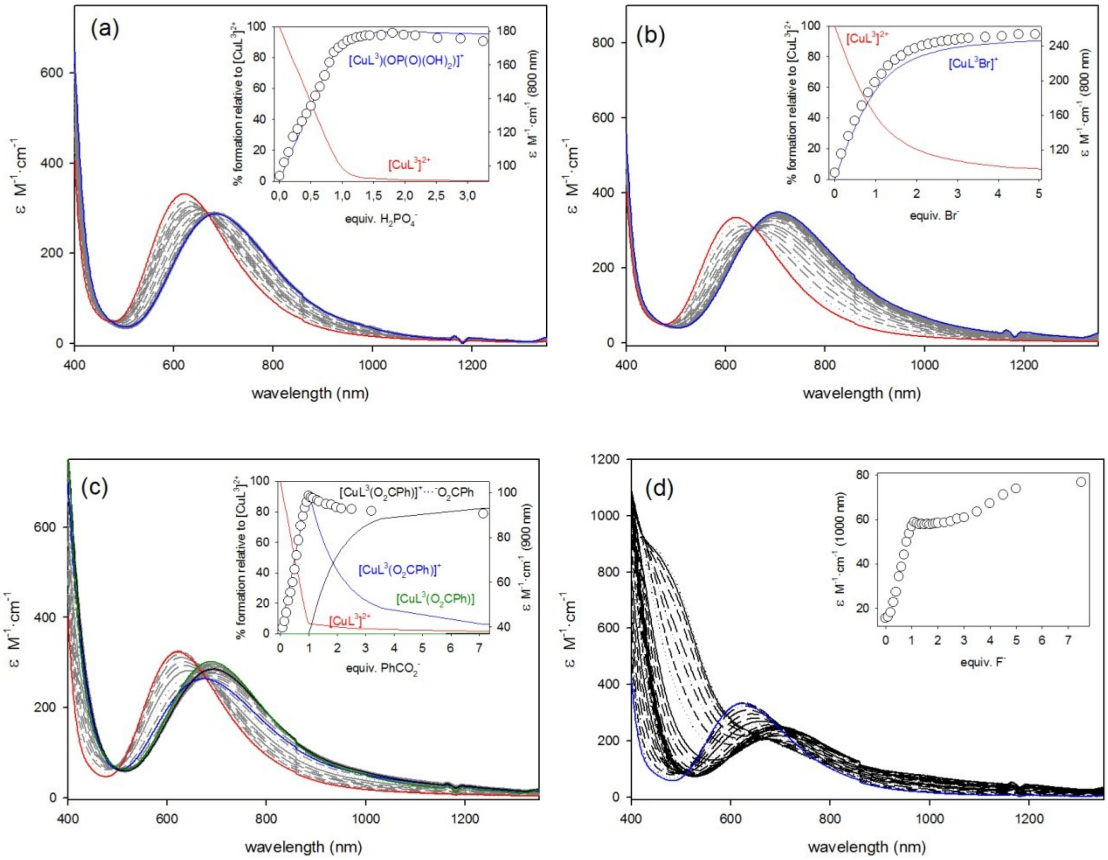

Figure S5. Family of UV/vis spectra recorded during the titration of $[CuL^3(OSMe_2)]^{2+}$ (10^{-3} M in dsmo) with a standard solution (0.1 M in dmso, 25 °C): (a) $[Bu_4N]\cdot H_2PO_4$; (b) $[Bu_4N]\cdot Br$; (c) $[Bu_4N]\cdot PhCO_2$; (d) $[Bu_4N]\cdot F$. Insets: titration profiles at selected wavelengths *vs* equivalents of anion and species distribution diagram (coordinated dmso molecules were omitted for the sake of simplicity).

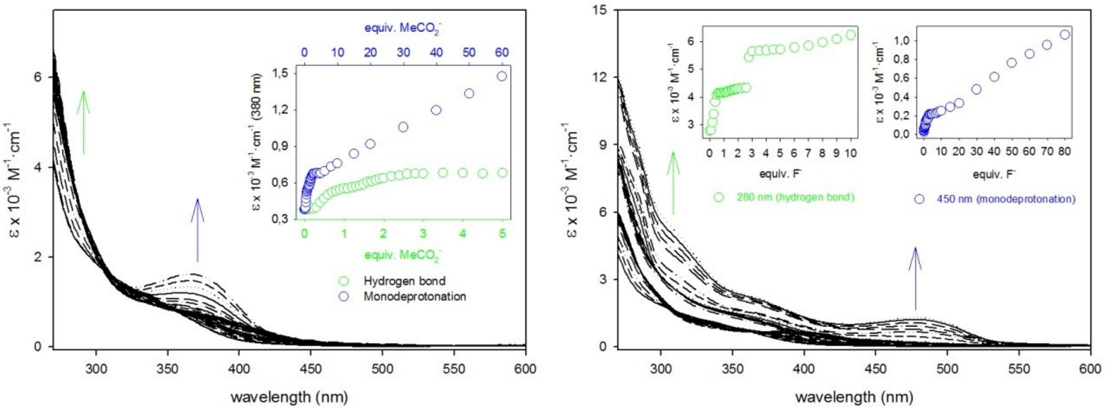

Figure S6. Family of UV/vis spectra recorded during the titrations of $[CuL^3(OSMe_2)]^{2+}$ (10^{-4} M in dmso) with standard solutions of $[Bu_4N]\cdot MeCO_2$ (left) and $[Bu_4N]\cdot F$ (right) (10^{-2} M in DMSO, 25 °C). Inset: titration profiles at a selected wavelength *vs.* equivalents of anion.

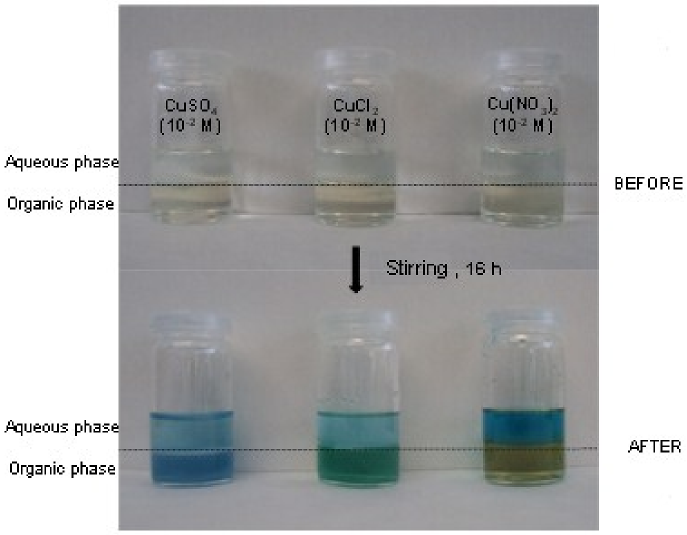

Figure S7. Preliminary solvent extraction studies with L^2 (10^{-2} M) and the copper salts: $CuSO_4$, $CuCl_2$ and $Cu(NO_3)_2$. A different extracting ability is suggested in each case by the colour intensity of the organic phase.

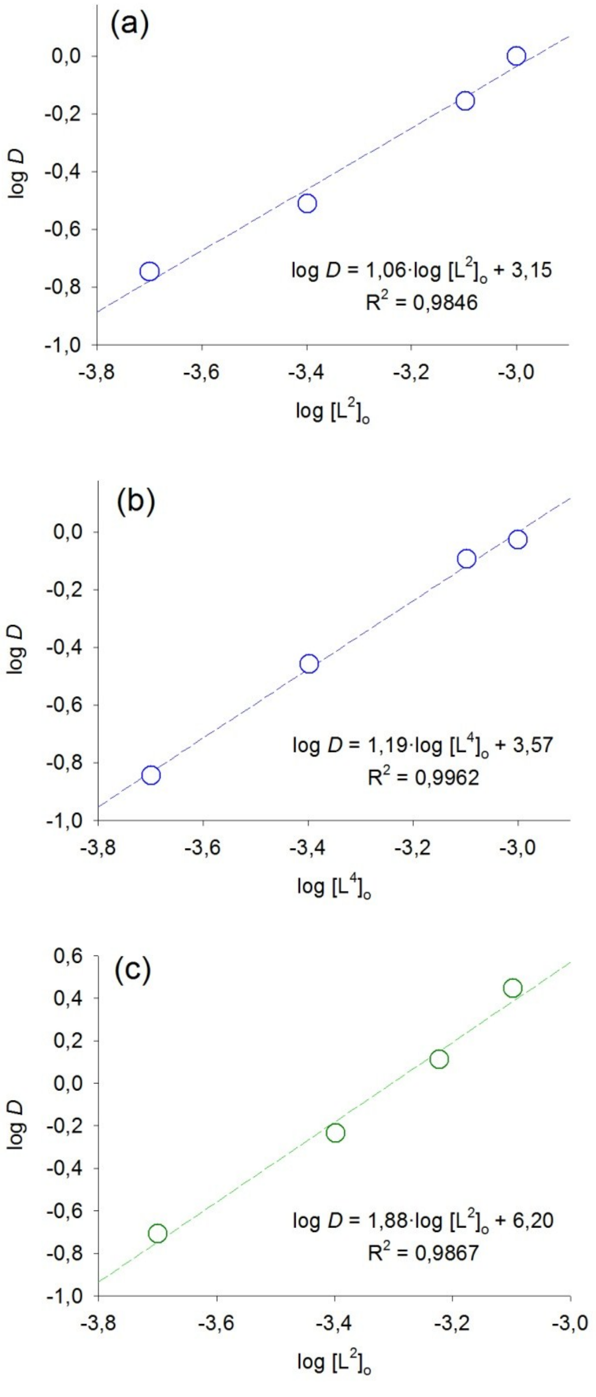

Figure S8. Log *D vs* log$[L^n]_o$ plots: $[CuSO_4]$: 10^{-3} M; $[Na_2SO_4]$: 0.6 M; $[CuCl_2]$: 10^{-3} M; [NaCl]: 0.6 M; pH: 5.5; slopes: (a) $[CuSO_4]$:$\mathbf{L^2}$ = 1.06; (b) $[CuSO_4]$:$\mathbf{L^4}$ = 1.19; (c) $[CuCl_2]$:$\mathbf{L^2}$ = 1.88.

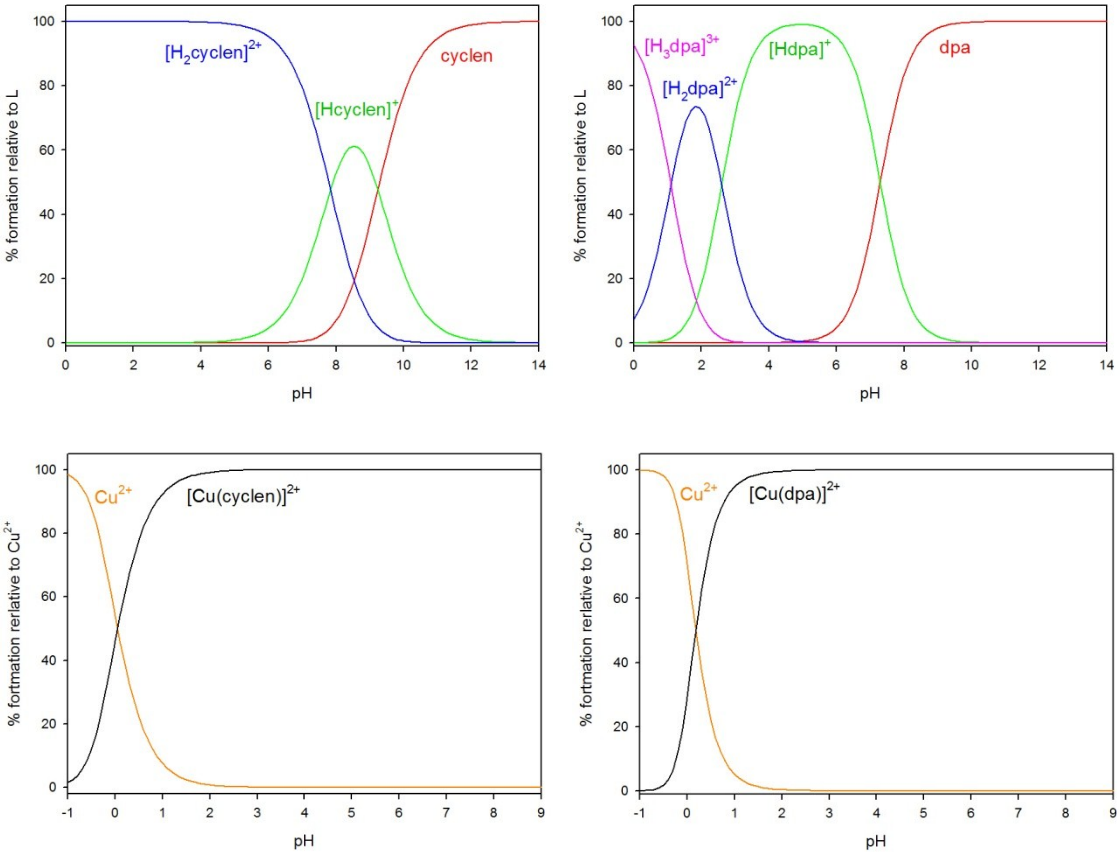

Figure S9. Speciation plots created from calculated acid dissociation constants for cyclen and dpa (top) and species distribution of the Cu(cyclen) and Cu(dpa) systems, 1:1 Cu(II)/L; 0.1 M $NaNO_3$ and KNO_3, respectively at 25 °C (bottom).

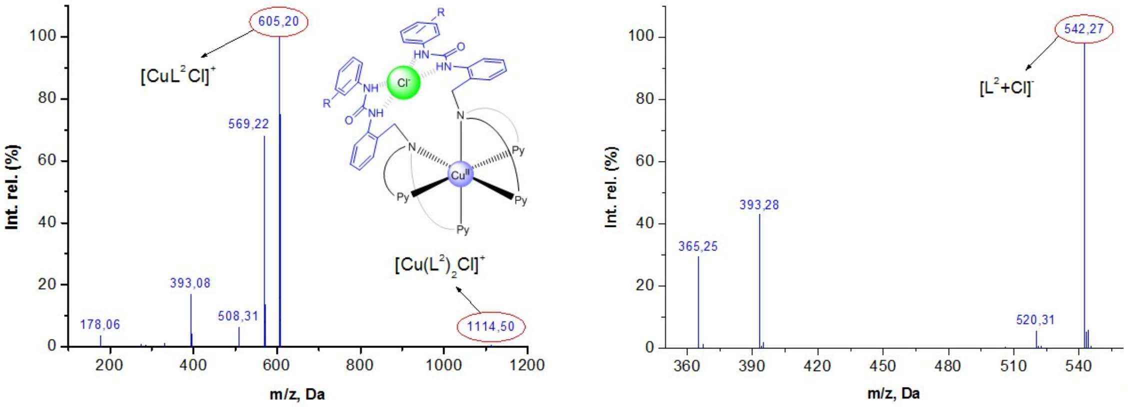

Figure S10. Mass spectra of the organic phase recorded after the solvent extraction of $CuCl_2$ with **L^2** showing the different species present in solution: [Cu**L^2**Cl]$^+$ and [Cu(**L^2**)$_2$Cl]$^+$ (ESI$^+$, left) and [**L^2**+Cl]$^-$ (ESI$^-$, right).

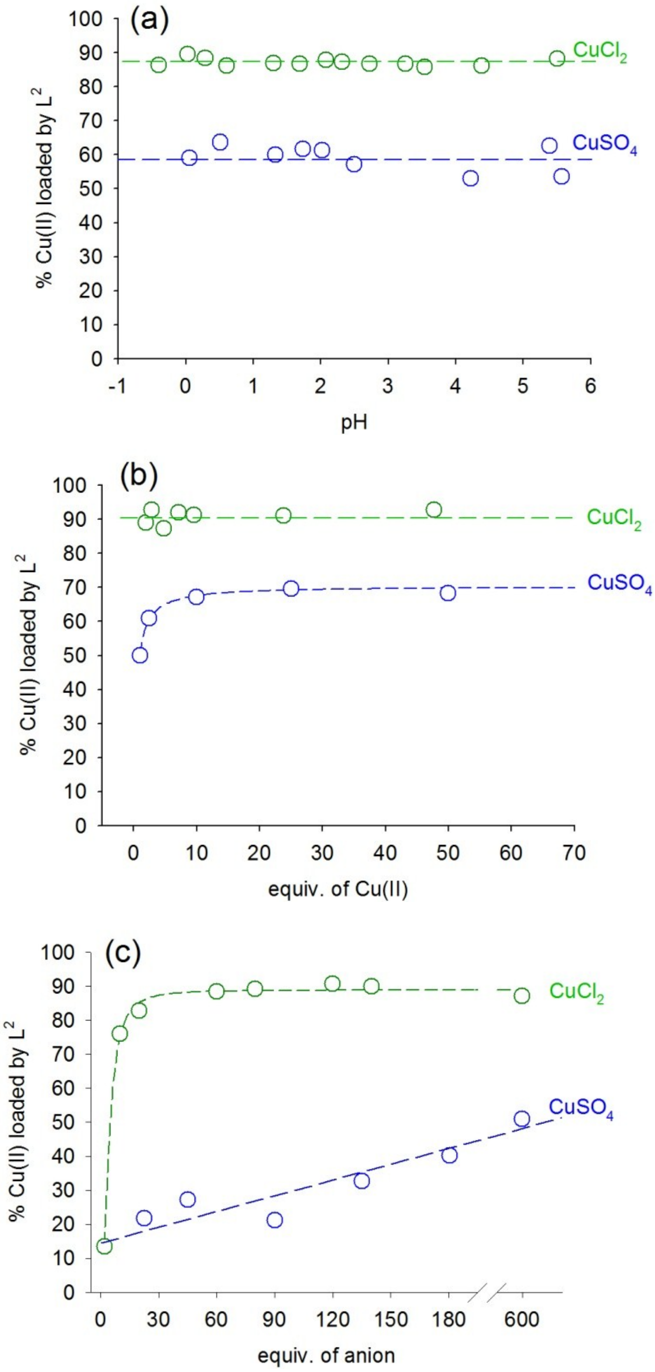

Figure S11. Loadings of $CuCl_2$ and $CuSO_4$ by $\mathbf{L^2}$ as a function of (a) the pH, (b) the Cu(II) concentration and (c) the anion concentration in the aqueous feed solution.

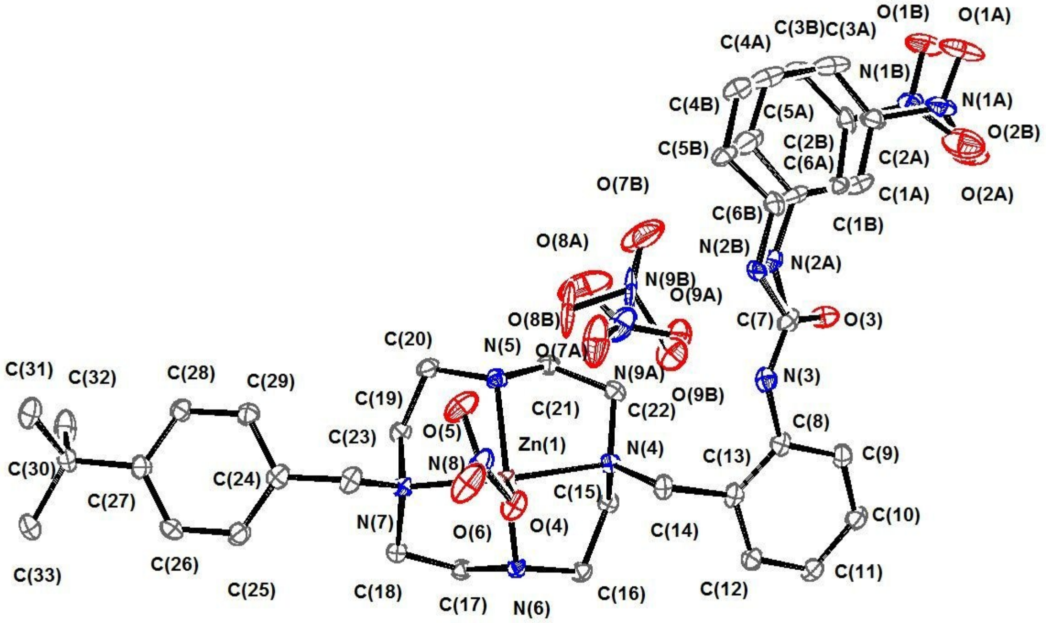

Figure S12. Single crystal X-ray structure of $[Zn\mathbf{L}^3(NO_3)_2]$ showing the disorder of the uncoordinated nitrate anion and the urea moiety.

Table S1. Bond distances (Å) and angles (°) of metal coordination environments in $[\mathrm{Cu}\mathbf{L}^3(\mathrm{SO}_4)]$, $[\mathrm{Zn}\mathbf{L}^3(\mathrm{NO}_3)]\mathrm{NO}_3$ and $[\mathrm{Cu}\mathbf{L}^1(\mu\text{-}\mathrm{SO}_4)]_2$ (see Fig. 2, Fig. 3 and Fig. 4 for numbering scheme).

	$[\mathrm{Cu}\mathbf{L}^3(\mathrm{SO}_4)]$	$[\mathrm{Zn}\mathbf{L}^3(\mathrm{NO}_3)]\mathrm{NO}_3$	$[\mathrm{Cu}\mathbf{L}^1(\mu\text{-}\mathrm{SO}_4)]_2$
M(1)-N(3)			3.007(1)
M(1)-N(4)	2.083(2)	2.083(2)	2.032(2)
M(1)-N(5)	2.001(2)	2.088(3)	1.998(2)
M(1)-N(6)	2.019(2)	2.093(2)	1.980(2)
M(1)-N(7)	2.071(2)	2.188(3)	
M(1)-O(4)	2.150(1)	1.989(2)	1.939(1)
M(1)-O(5)			
M(1)-O(7)			2.327(1)*
N(4)-M(1)-N(5)	86.84(6)	82.4(1)	81.74(6)
N(4)-M(1)-N(6)	84.06(7)	81.9 (1)	83.78(6)
N(4)-M(1)-N(7)	150.76(7)	142.76(9)	
N(4)-M(1)-O(4)	103.32(6)	107.20(9)	163.50(6)
N(4)-M(1)-O(5)			
N(4)-M(1)-O(7)			90.01(6)[a]
N(5)-M(1)-N(6)	146.13(7)	133.8(1)	165.33(7)
N(5)-M(1)-N(7)	85.97(6)	84.0(1)	
N(5)-M(1)-O(4)	101.45(6)	120.0(1)	90.72(6)
N(5)-M(1)-O(5)			
N(5)-M(1)-O(7)			90.20(6) [a]
N(6)-M(1)-N(7)	86.29(7)	82.93(9)	
N(6)-M(1)-O(4)	112.38(6)	106.1(1)	103.88(6)
N(6)-M(1)-O(5)			
N(6)-M(1)-O(7)			87.45(6) [a]
N(7)-M(1)-O(4)	105.88(6)	109.7(1)	
O(4)-M(1)-O(5)			
O(4)-M(1)-O(7)			104.75(5) [a]

[a] Symmetry transformation used to generate equivalent atoms (O7#1) in $[\mathrm{Cu}\mathbf{L}^1(\mu\text{-}\mathrm{SO}_4)]_2$: -x+1, -y+1, -z+1.

Scheme S1. Chemical structures of the ligands $\mathbf{L}^{1\text{-}4}$ investigated in this work.